Atmos. Chem. Phys., 22, 4827–4839, 2022
https://doi.org/10.5194/acp-22-4827-2022

Atmospheric Chemistry and Physics
Open Access
EGU

The optical properties and in-situ observational evidence for the formation of brown carbon in clouds

Ziyong Guo[1,2,3], Yuxiang Yang[1,2,3], Xiaodong Hu[1,2,3], Xiaocong Peng[1,2,3], Yuzhen Fu[1,2,3], Wei Sun[1,2,3], Guohua Zhang[1,3,4], Duohong Chen[5], Xinhui Bi[1,3,4], Xinming Wang[1,3,4], and Ping'an Peng[1,3,4]

[1]State Key Laboratory of Organic Geochemistry and Guangdong Provincial Key Laboratory of Environmental Protection and Resources Utilization, Guangzhou Institute of Geochemistry, Chinese Academy of Sciences, Guangzhou 510640, PR China
[2]University of Chinese Academy of Sciences, Beijing 100049, PR China
[3]CAS Center for Excellence in Deep Earth Science, Guangzhou 510640, PR China
[4]Guangdong-Hong Kong-Macao Joint Laboratory for Environmental Pollution and Control, Guangzhou Institute of Geochemistry, Chinese Academy of Sciences, Guangzhou 510640, PR China
[5]State Environmental Protection Key Laboratory of Regional Air Quality Monitoring, Guangdong Environmental Monitoring Center, Guangzhou 510308, PR China

Correspondence: Guohua Zhang (zhanggh@gig.ac.cn)

Received: 11 November 2021 – Discussion started: 25 November 2021
Revised: 22 February 2022 – Accepted: 9 March 2022 – Published: 12 April 2022

Abstract. Atmospheric brown carbon (BrC) makes a substantial contribution to aerosol light absorption and thus global radiative forcing. Although BrC may change the lifetime of the clouds and ultimately affect precipitation, little is known regarding the optical properties and formation of BrC in the clouds. In the present study, the light-absorption properties of cloud droplet residual (cloud RES) were measured by coupled a ground-based counterflow virtual impactor (GCVI) and an aethalometer (AE-33), in addition to the cloud interstitial (cloud INT) and ambient (cloud-free) particles by $PM_{2.5}$ inlet-AE-33 at Mt. Tianjing (1690 m a.s.l.), a remote mountain site in southern China, from November to December 2020. Meanwhile, the light-absorption and fluorescence properties of water-soluble organic carbon (WSOC) in the collected cloud water and $PM_{2.5}$ samples were also obtained, associated with the concentration of water-soluble ions. The mean light-absorption coefficient (Abs_{370}) of the cloud RES, cloud INT, and cloud-free particles were 0.25 ± 0.15, 1.16 ± 1.14, and $1.47 \pm 1.23\ Mm^{-1}$, respectively. The Abs_{365} of WSOC was $0.11 \pm 0.08\ Mm^{-1}$ in cloud water and $0.40 \pm 0.31\ Mm^{-1}$ in $PM_{2.5}$, and the corresponding mass absorption efficiency (MAE_{365}) was 0.17 ± 0.07 and $0.31 \pm 0.21\ m^2\ g^{-1}$, respectively. A comparison of the light-absorption coefficient between BrC in cloud RES and cloud INT particles, and WSOC in cloud water and $PM_{2.5}$ indicates a considerable contribution (48 %–75 %) of water-insoluble BrC to total BrC light absorption. Secondary BrC estimated by minimum R squared (MRS) method dominated the total BrC in cloud RES (67 %–85 %), rather than in the cloud-free (11 %–16 %) and cloud INT (9 %–23 %) particles. It may indicate the formation of secondary BrC during cloud processing. Supporting evidence includes the enhanced WSOC and dominant contribution of the secondary formation and biomass burning factor (>80 %) to Abs_{365} in cloud water provided by positive matrix factorization (PMF) analysis. In addition, we showed that the light absorption of BrC in cloud water was closely related to humic-like substances and tyrosine-like and/or protein-like substances ($r > 0.63$, $p < 0.01$), whereas only humic-like substances for $PM_{2.5}$, as identified by excitation-emission matrix fluorescence spectroscopy.

Highlights.

- The optical properties of BrC in both cloud-processed and cloud-free particles were simultaneously obtained.
- An in-cloud process may facilitate the formation of BrC, with secondary BrC as the dominant fraction (67 %–85 %).
- Light absorption of BrC in cloud water is closely related to humic-like and tyrosine-like and/or protein-like substances.

1 Introduction

Brown carbon (BrC) makes a significant contribution to global radiative forcing, equivalent to 27 %–70 % of that from black carbon (BC) (G. Lin et al., 2014). The addition of BrC in climate models may change the direct radiation effect of organic aerosols from cooling ($-0.08\,W\,m^{-2}$) to warming ($+0.025\,W\,m^{-2}$), which may affect the lifetime and distribution of clouds, and thus precipitation and surface temperature (Zhuang et al., 2010). BrC may also contribute to uncertainties in global radiative forcing, as estimated to cause positive radiative forcing (-2.0 to $+2.5\,W\,m^{-2}$, with an average of $0.01 \pm 0.04\,W\,m^{-2}$) in aerosol-cloud interaction (Brown et al., 2018). However, such models rarely considered the secondary BrC, although increasing evidence shows that secondary BrC may represent the dominant fraction of total BrC (19 %–91 %) (Wang et al., 2019a, b).

Aqueous-phase reactions in the clouds have been shown to significantly affect global secondary organic aerosol (SOA) production (Ervens, 2015; Liu et al., 2012; Spracklen et al., 2011), and thus may potentially contribute to secondary BrC. Production of BrC from aqueous-phase reactions has been extensively investigated in the laboratory, revealing that BrC can also be formed secondarily through a variety of mechanisms, e.g., photochemical oxidation, nitration, and Maillard reactions (Y. H. Lin et al., 2014; Pósfai et al., 2004; Shapiro et al., 2009). For instance, secondary BrC is observed from the photo-oxidation of aromatics (Pang et al., 2019; J. Yang et al., 2021), the nitration of phenol (Heal et al., 2007; Vione et al., 2001), and the reaction of carbonyls with ammonium or amines (De Haan et al., 2011; Nguyen et al., 2012; Heal et al., 2007). Secondary BrC such as nitrophenols, aromatic carbonyls, imidazole, and organosulfates have also been detected in cloud and fog water (Desyaterik et al., 2013; Kim et al., 2019; Pratt et al., 2013; Bianco et al., 2016a; Lebedev et al., 2018; Lüttke and Levsen, 1997). However, to what extent in-cloud processes contribute to the formation of BrC is still unclear.

Given that the currently applied imaginary refractive index of BrC based on the empirical formula of BC to OA ratio (Saleh et al., 2014) in the model simulation (Brown et al., 2018) may induce potential bias (Bikkina and Sarin, 2019), more field studies should be conducted to constrain the optical properties of BrC. Although various light-absorbing species have been identified in clouds, only a few studies focused on the optical properties of BrC in fog and clouds. Nitrophenols and aromatic carbonyls were the major fraction contributing to the light absorption (~ 50 %) of cloud water at wavelengths from 300 to 400 nm at Mt. Tai (Desyaterik et al., 2013). The mass absorption efficiency (MAE_{365}) of water-soluble organic carbon (WSOC) in fog water in California was 0.1–0.6 $m^2\,g^{-1}$ (Kaur and Anastasio, 2017). Many field studies focused on the optical properties of BrC in particulate matter. The light absorption of BrC in $PM_{2.5}$ was well correlated with nitrophenols, polycyclic aromatic hydrocarbons, and oxygenated polycyclic aromatic hydrocarbons (Wu et al., 2020). Nitrophenols and carbonyl oxygenated polycyclic aromatic hydrocarbons accounting 10 %–14 % to the light absorption at 365 nm in urban $PM_{2.5}$ (Huang et al., 2020). The contribution of nitrophenols and nitrated salicylic acids to the aqueous extract light absorption of PM_{10} was 0.10 %–3.71 % and five times higher than their mass contribution to WSOC (Teich et al., 2017). The fluorescent chromophores of fog and cloud water, as identified by excitation-emission matrix fluorescence spectroscopy (EEMs) in Louisiana and at Mt. Tai, were mainly composed of humic-like and protein-like substances (Birdwell and Valsaraj, 2010; Zhao et al., 2019), which might also be related to the presence of BrC (Chen et al., 2016; H. Wang et al., 2020). However, such studies were generally limited to $PM_{2.5}$, rather than in the clouds.

Our previous studies showed that the in-cloud aqueous-phase reactions could significantly promote the formation of SOA, such as nitrogen-containing organic matters, and affect the physicochemical properties of particles (Fu et al., 2020; Lian et al., 2021; Lin et al., 2017; Zhang et al., 2017a). In the present study, we took a further step to perform simultaneous on-line measurements of the light-absorption coefficients for the cloud droplet residual (cloud RES), cloud interstitial (cloud INT), and ambient (cloud-free) particles, coupled with the light-absorption and concentration measurements of WSOC in cloud water and $PM_{2.5}$. We aim to explore: (1) the optical properties of BrC in cloud-processed, cloud-free particles and WSOC in $PM_{2.5}$ and cloud water; (2) the possible contribution of in-cloud production to BrC light absorption, and (3) the characteristics of fluorescent chromophores in cloud water and $PM_{2.5}$ and their relationship with light-absorption properties of BrC.

2 Methods

2.1 Sampling setup

Measurements of the cloud-free, cloud RES, and cloud INT particles were performed at Mt. Tianjing (24°41′56″ N, 112°53′56″ E, 1690 m a.s.l.) in Guangdong province, China between 18 November and 5 December 2020. This site is located at a national forest reserve and is less affected by anthropogenic sources. The cloud event determination threshold was set as visibility less than 3 km and relative humidity (RH) larger than 95 %. During the cloud events, the cloud

RES and cloud INT particles were alternately introduced into the instruments through a ground-based counterflow virtual impactor (GCVI, model 1205, Brechtel Mfg., Inc., USA) and $PM_{2.5}$ cutoff, respectively, at a frequency of 1 hour. The GCVI cut size was set to 7.5 µm, where the transmission efficiency of cloud droplets was 50 % (Shingler et al., 2012). It should be noted that the $PM_{2.5}$ inlet may introduce possible uncertainty for the collection of cloud INT particles due to the interference of cloud droplets, although the size distribution of cloud droplets was mainly concentrated on 6–9 µm at mountain sites (Li et al., 2017). However, this would not be the case when cloud residual particles are mainly focused on, as in the present study. The collected cloud droplets passed through an evaporation chamber (40 °C), resulting in the cloud RES particles for downstream analysis. An aethalometer (model AE-33, Magee Scientific., USA) was used to measure the light-absorption coefficients of particles at wavelengths of 370, 470, 520, 590, 660, 880, and 950 nm. AE-33 uses two parallel spot measurement technologies to compensate for the light attenuation due to the filter loading effect (Drinovec et al., 2015). The BC concentration was calculated by the light-absorption coefficient at 880 nm. The detection limit of BC is less than 10 ng m^{-3} (equal to 0.077 Mm^{-1} at 880 nm) and the uncertainty is ∼ 2 ng m^{-3} (equal to 0.015 Mm^{-1} at 880 nm), with a time resolution of 1 min.

Cloud water samples were collected by a Caltech Active Strand Cloud Water Collector, Version 2 (CASCC2) (Demoz et al., 1996; Y. Yang et al., 2021) when the visibility was less than 200 m (from 14 November to 4 December 2020). The cut size was 3.5 µm, the flow rate was 5.8 m^3 min^{-1}, and the overall collection efficiency was 86 %. During the sampling period, 53 cloud water samples were collected. The 0.22 µm quartz fiber filter was used immediately to remove insoluble components after collection of cloud water and then frozen at −20 °C until analysis. Meanwhile, $PM_{2.5}$ samples were collected by a mid-volume (300 L min^{-1}) aerosol sampler (PM-PUF-300, Mingye, China). Daily samples (during 14 November to 8 December 2020) were collected on the quartz fiber filters, which were prebaked at 450 °C for 4 h in a muffle furnace to remove residual organics before use. After collection, all samples were frozen at −20 °C until analysis. In this study, $PM_{2.5}$ samples collected at the same time as cloud water samples were regarded as INT-$PM_{2.5}$ ($n = 13$), and the others as FREE-$PM_{2.5}$ ($n = 19$). It should be noted that some FREE-$PM_{2.5}$ samples also experienced short cloud events during collection. Blank samples of the cloud water and $PM_{2.5}$ were collected and processed following the same procedure as the samples.

2.2 Calculation of secondary BrC light absorption

The light-absorption coefficient ($Abs_{BrC}(\lambda)$, Mm^{-1}) of BrC in different wavelengths can be obtained by AE-33, assuming that the absorption Ångström exponent (AAE) of BC is 1 and the light absorption at 880 nm only due to BC (Drinovec et al., 2015). The cloud RES, cloud INT, and cloud-free particles were generally located in submicron size (Fig. S1), and thus were unlikely to have originated from noncombustion sources and are mostly biogenic and mainly exist in the coarse mode (Perrino and Marcovecchio, 2016). The $Abs_{BrC}(\lambda)$ contributed by the combustion sources can be estimated through a BC-tracer method (Wu et al., 2018)

$$\mathrm{Abs}_{\mathrm{pri,comb}}(\lambda) = \left(\frac{\mathrm{Abs}(\lambda)}{\mathrm{BC}}\right)_{\mathrm{pri}} \times [\mathrm{BC}]. \quad (1)$$

Where $\mathrm{Abs}(\lambda)$ is the total light-absorption coefficient of carbonaceous aerosol that was measured by AE-33, $(\frac{\mathrm{Abs}(\lambda)}{\mathrm{BC}})_{\mathrm{pri}}$ can be determined by the minimum R squared (MRS) method to further evaluate the relative contribution of primary BrC and secondary formation BrC to the overall $\mathrm{Abs}_{\mathrm{BrC}}(\lambda)$. Firstly, $\mathrm{Abs}_{\mathrm{pri,comb}}(\lambda)$ is calculated based on $(\frac{\mathrm{Abs}(\lambda)}{\mathrm{BC}})_{\mathrm{pri}}$, which is assumed to be step increasing from 0 to 120 with a rate of 0.1. The target $(\frac{\mathrm{Abs}(\lambda)}{\mathrm{BC}})_{\mathrm{pri}}$ value can be retrieved when the correlation coefficient (R^2) between $\mathrm{Abs}_{\mathrm{BrC,sec}}(\lambda)$ with BC concentration reaching the minimum (see Fig. S2). Previous studies showed that the bias of MRS method is less than 23 % when the measurement uncertainty is less than 20 % (Wu and Yu, 2016). It should be noted that when the measured ratio of $\frac{\mathrm{Abs}(\lambda)}{\mathrm{BC}}$ is lower than the retrieved $(\frac{\mathrm{Abs}(\lambda)}{\mathrm{BC}})_{\mathrm{pri}}$, the $\mathrm{Abs}_{\mathrm{BrC,sec}}(\lambda)$ could be negative. In these cases, $\mathrm{Abs}_{\mathrm{BrC,sec}}(\lambda)$ is set to zero for subsequent analysis (Kaskaoutis et al., 2021; Wang et al., 2019a). These cases account for less than 5 % in the cloud RES and 28 %–70 % in the cloud INT and cloud-free particles

2.3 Measurements of $PM_{2.5}$ and cloud water

$PM_{2.5}$ samples were ultrasonically extracted with ultrapure water (resistivity: 18.2 MΩ cm) for 30 min, then filtered by 0.22 µm polytetrafluoroethylene (PTFE) filters to obtain the $PM_{2.5}$ aqueous extract. The concentrations of water-soluble ions, water-soluble heavy metals, WSOC in $PM_{2.5}$ aqueous extract and cloud water samples were analyzed by ion chromatography (Metrohm 883 IC plus, Switzerland), inductively coupled plasma mass spectrometry (ICP-MS, Thermo Fisher, USA), and total organic carbon analyzer (TOC-V, Shimadzu, Japan), respectively. Parallel analyses showed that the relative standard deviation of each analysis was generally less than 15 %. The reported concentration data herein was after blank subtraction.

The light-absorption coefficient ($\mathrm{Abs}_{\mathrm{WSOC},\lambda}$) of WSOC can be obtained (Hecobian et al., 2010) by the measurement of cloud water and $PM_{2.5}$ aqueous extract, with UV-Vis (UV1901, Kejie, China)

$$\mathrm{Abs}_{\mathrm{WSOC},\lambda} = (A_\lambda - A_{700}) \times \frac{V_{\mathrm{l}}}{V_{\mathrm{a}} \times L} \times \ln(10). \quad (2)$$

Where A_λ is the absorbance of the sample, A_{700} is used to account for any drift; V_{l} is the volume of ultrapure water used

to extract the sample (for cloud water it is the total sample volume), V_a is the volume of sampled air through the PTFE filter (for cloud water it is the total volume of sampled air), and L is the cuvette path length (0.01 m).

The AAE values describing the spectral dependence of WSOC light absorption can be further deduced by exponential fitting $Abs_{WSOC,\lambda}$ between 300–500 nm. The $MAE_{WSOC,\lambda}$ can be calculated by dividing $Abs_{WSOC,\lambda}$ by the mass concentration of WSOC ($\mu g\,m^{-3}$). The E_{250}/E_{365} (the ratio of absorbance at 250 nm to that at 365 nm) is used to describe the humification of organic matter, which is inversely related to aromaticity and molecular weight of WSOC (Kristensen et al., 2015). Specific UV absorbance (SUVA, $m^2\,g^{-1}$) at 254 and 280 nm has been proved to be qualitatively related to the structural characteristics (aromaticity and molecular weight) of WSOC to a certain extent (Weishaar et al., 2003), which can be calculated using the following equation:

$$SUVA_{254\text{ or }280} = \frac{A}{L \times C_{WSOC}}, \quad (3)$$

where A is the absorbance of sample at 254 or 280 nm and C_{WSOC} is the concentration of WSOC ($mg\,L^{-1}$).

The excitation-emission matrix fluorescence spectroscopy (EEMs) of $PM_{2.5}$ extract and cloud water was measured by a fluorescence spectrophotometer (F97pro, Lengguang, China). The sample blank was deducted before analysis, and the EEMs were normalized to the Raman units (R.U.) by using the Ramen peak (Ex = 350 nm, Em = 365–430 nm) of ultrapure water measured simultaneously with the sample (Lawaetz and Stedmon, 2009). Parallel factor (PARAFAC) analysis was performed on the acquired spectra with drEEM toolbox (version 0.3.0) based on MATLAB (Murphy et al., 2013). According to the outlier tests of PARAFAC, six samples with high leverage and high residual signals were removed in the modeling of $PM_{2.5}$ aqueous extract. The details for obtaining maximum fluorescence intensity (F_{max}), fluorescence index (FI), recent autochthonous contribution (BIX), and humification index (HIX) were described in Sect. S1 in the Supplement.

3 Results and discussion

3.1 The optical properties of BrC during cloud events

The presence of BrC could be indicated by the AAE values derived from AE-33 data, which are 1.30 ± 0.12 for cloud-free, 1.36 ± 0.22 for cloud INT, and 1.32 ± 0.15 for cloud RES particles. The light-absorption coefficient of BrC at 370 nm (Abs_{370}) of cloud-free, cloud INT and cloud RES particles are 1.47 ± 1.23, 1.16 ± 1.14, and $0.25 \pm 0.15\,Mm^{-1}$, respectively (Fig. 1), with the AAE values of BrC at 2.71 ± 0.69, 3.13 ± 0.97, and 2.76 ± 0.89, respectively. The contribution of BrC light absorption to the total particle light absorption in the cloud-free, cloud INT, and cloud RES particles shows no significant difference, on average decreasing from ~ 23 % at 370 nm to ~ 7 % at 660 nm, as shown in Fig. 2.

For the cloud water and $PM_{2.5}$ aqueous extracts, light absorption properties of WSOC at 365 nm are taken as the representative to those of water-soluble BrC (WS-BrC) in the present study. As expected, there is a positive correlation between Abs_{365} and WSOC concentration in both cloud water and $PM_{2.5}$ aqueous extracts ($r > 0.61$, $p < 0.01$). As shown in Fig. 1, there is great difference in Abs_{365} of WSOC in FREE-$PM_{2.5}$, INT-$PM_{2.5}$, cloud water-Day, and cloud water-Night, which are 0.49 ± 0.34, 0.27 ± 0.18, 0.09 ± 0.04, and $0.13 \pm 0.10\,Mm^{-1}$, respectively. The Abs_{365} of WSOC in $PM_{2.5}$ in this study is at the same magnitude as that of PM_{10} in the Tibetan Plateau (Kirillova et al., 2016), and much lower than those in urban areas (3.4–33.9 Mm^{-1}, as summarized in Table S1) (Chen et al., 2018, 2020; Huang et al., 2020; Kim et al., 2016). The AAE of WSOC has no significant difference among FREE-$PM_{2.5}$, INT-$PM_{2.5}$, cloud water-Day, and cloud water-Night, which are 6.01 ± 0.81, 5.37 ± 1.08, 5.81 ± 1.47, and 6.31 ± 1.51, respectively, within the reported range.

The MAE_{365} of WSOC in FREE-$PM_{2.5}$, INT-$PM_{2.5}$, cloud water-Day, and cloud water-Night are 0.31 ± 0.17, 0.31 ± 0.26, 0.17 ± 0.07, and $0.17 \pm 0.07\,m^2\,g^{-1}$, respectively. The MAE_{365} of WSOC in cloud water and $PM_{2.5}$ are much lower than those in urban and alpine areas, and various source emission samples (Table S1) (Chen et al., 2018, 2020; Fan et al., 2016; Huang et al., 2020; Kim et al., 2016; Kirillova et al., 2016; Li et al., 2019; Park and Yu, 2016; Soleimanian et al., 2020; Wu et al., 2019). The MAE_{365} of WSOC shows no significant difference between the FREE-$PM_{2.5}$ and INT-$PM_{2.5}$, which is similar to the result observed in the Indo-Gangetic Plain (Choudhary et al., 2018), but their values are quite a bit higher, i.e., 1.6 and $1.8\,m^2\,g^{-1}$ for the INT-$PM_{1.0}$ and FREE-$PM_{1.0}$, respectively. The MAE_{365} of WSOC in cloud water (0.06–0.32 $m^2\,g^{-1}$) is slightly lower than the previously reported values in fog water (0.1–0.6 $m^2\,g^{-1}$) in California (Kaur and Anastasio, 2017). Both the MAE_{365} of WSOC in cloud water and $PM_{2.5}$ show a positive correlation ($r > 0.84$, $p < 0.01$) with $SUVA_{254/280}$, and a medium negative correlation ($r > 0.43$, $p < 0.05$) with E_{250}/E_{365}, which may indicate that a higher MAE_{365} of WSOC has a higher aromatic and molecular weight; the aromaticity and molecular weight of WSOC may influence the light absorption capacity of cloud water and $PM_{2.5}$ (Fig. S3).

Although there are tight correlations between the Abs_{370} for cloud water and the cloud RES particles, and for the INT-$PM_{2.5}$ and the cloud INT particles (Fig. 3, $r > 0.60$, $p < 0.01$), the Abs_{370} of WSOC in cloud water ($0.12\,Mm^{-1}$) and INT-$PM_{2.5}$ ($0.27\,Mm^{-1}$) are considerably lower than those in the cloud RES ($0.24\,Mm^{-1}$) and cloud INT particles ($1.08\,Mm^{-1}$) that collected simultaneously. Such differences may be attributed to the contribution of water-insoluble or-

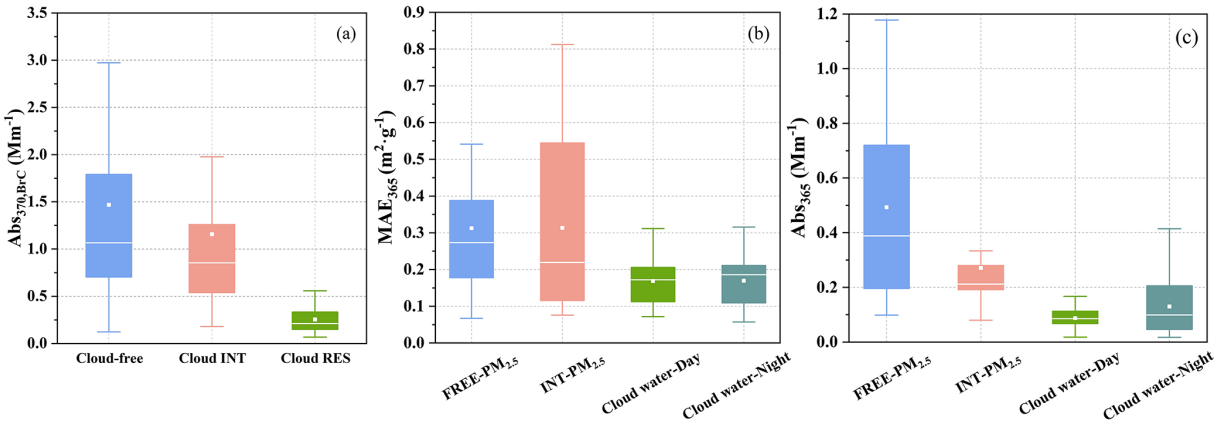

Figure 1. **(a)** The Abs_{370} of cloud-free, cloud INT, and cloud RES particles, and **(b)** the MAE_{365} and **(c)** Abs_{365} of FREE-$PM_{2.5}$, INT-$PM_{2.5}$, cloud water-Day, and cloud water-Night.

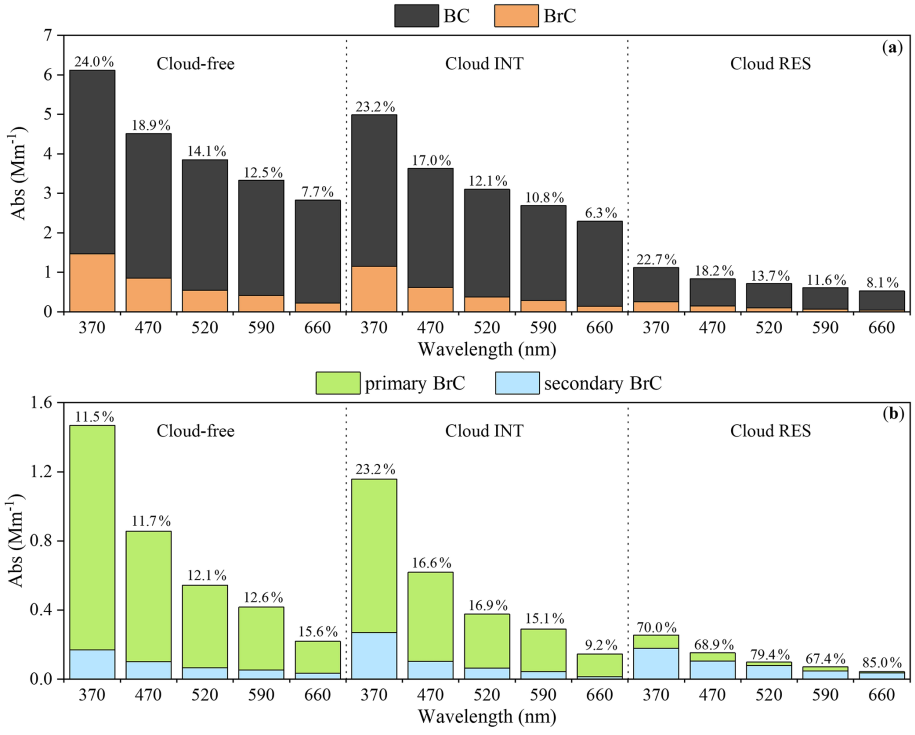

Figure 2. The light absorption of **(a)** BrC and BC; **(b)** primary BrC and secondary BrC at different wavelengths; the percentages represent the contribution of **(a)** BrC light absorption to the total particle light absorption; **(b)** secondary BrC light absorption to the total BrC light absorption in the cloud-free, cloud INT, and cloud RES particles, respectively.

ganic carbon (WIOC). The different optical properties for the whole BrC and WS-BrC may also be reflected by the AAE values. They are generally in the range of 4–8 at 300–500 nm in cloud water and $PM_{2.5}$, much higher than those for BrC (2–4) calculated from AE-33 data at 370–660 nm. The contribution of water-insoluble BrC to the light absorption is estimated to be ∼ 75 % for the cloud INT particles and ∼ 48 % for the cloud RES particles on average, based on these differences (Fig. 3). It is also noted that the light absorption of WIOC might still be underestimated by ∼ 16 % when sampling size is considered for the GCVI and cloud sampler (as discussed in Sect. S1). High contributions of WIOC to BrC light absorption have also been observed in the Indo-Gangetic Plain (77 %) (Satish et al., 2020), Beijing (62 %), and Xi'an (51 %) (Huang et al., 2020).

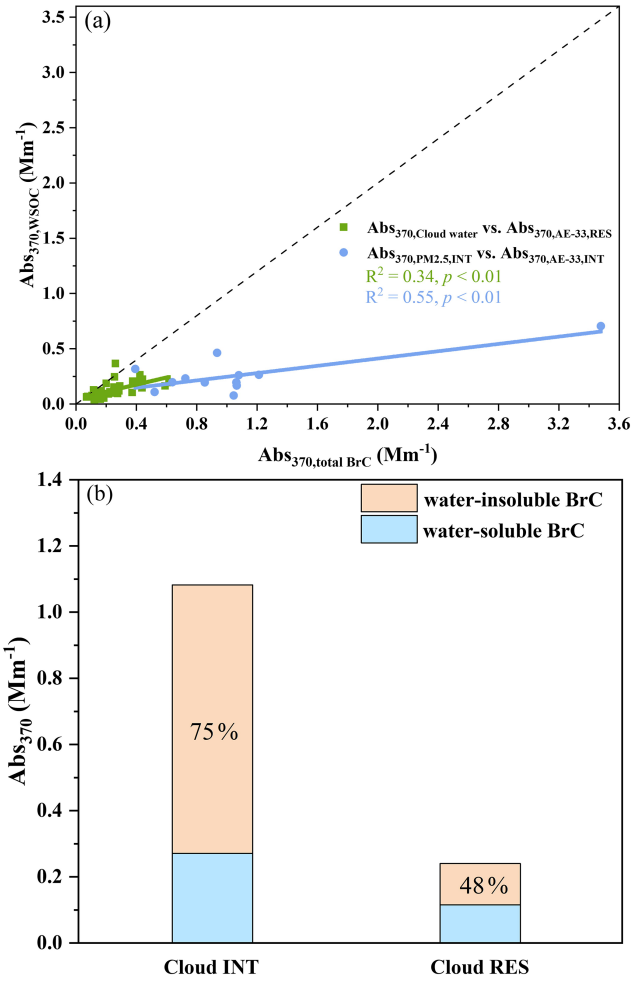

Figure 3. **(a)** The correlations of WSOC light absorption to total BrC light absorption in 370 nm, and **(b)** the contribution of water-soluble BrC and water-insoluble BrC to total BrC light absorption.

3.2 The secondary contribution of BrC during cloud events

Figure 2 shows the contribution of secondary BrC to the total BrC in cloud-free, cloud INT, and cloud RES particles estimated by the MRS method; 11 %–16 % and 9 %–23 % of the total absorption of BrC come from the secondary BrC for the cloud-free and cloud INT particles, respectively. Only a slight difference was observed for the cloud-free and cloud INT particles, indicating that cloud processing may have limited influence on the cloud INT particles. It is noted that even during the cloud-free periods, RH was generally higher than 70 % (Fig. S1). The contribution of secondary BrC in cloud INT and cloud-free particles are in the low range of reported values (as summarized in Table S2) (Gao et al., 2022; Kaskaoutis et al., 2021; Lin et al., 2021; Q. Wang et al., 2019a, b, 2020, 2021; Zhang et al., 2020, 2021; Zhu et al., 2021).

Differently, the contribution of secondarily formed BrC to the total BrC light absorption is 67 %–85 % in the cloud RES particles, which is surprisingly higher than those in the cloud-free and cloud INT particles. Such a high contribution may suggest how critical the role of cloud processing in the formation of BrC is. Compared with the relative contributions for the cloud-free and cloud INT particles, the importance of such a process in cloud droplets remarkably overrides that in cloud-free and cloud INT particles. The significance of secondary water-soluble BrC formation in cloud droplets may also be reflected by the significant correlation between the Abs_{365} of cloud water and $PM_{2.5}$ aqueous extract with SNA (sulfate, nitrate, and ammonium) ($r>0.77$, $p<0.01$), and NO_x ($r>0.58$, $p<0.01$), as shown in Fig. S4. The SNA and NO_x concentrations are higher at night than in the daytime (Fig. S5), which is consistent with higher Abs_{365} of cloud water at night. NO_2^- resulting from dissolved NO_x can react with benzene and finally forms nitrophenol in the presence of UV-A (Harrison et al., 2005; Vione et al., 2004). Various of reactive oxygen and nitrogen species generated from the photolysis of inorganic nitrate in aqueous-phase could also facilitate the photooxidation of organic compounds to form BrC (Seinfeld and Pandis, 2016; J. Yang et al., 2021) and potentially contribute to the light absorption of cloud water (Desyaterik et al., 2013). In-cloud aqueous processes leading to more CHON compounds in cloud water than below-cloud atmospheric particles have also been observed (Boone et al., 2015). In addition, a comparison between the WSOM ($WSOM = WSOC \times 1.8$) normalized by K^+ (as a primary source tracer) in cloud water and INT-$PM_{2.5}$ (Fig. S6) also clearly indicates the enhanced formation of WSOM in cloud water. It is consistent with that the light absorption of WSOC contributed more to the cloud RES ($\sim$ 52 %) than the cloud INT (25 %) particles, as estimated in Fig. 3.

The source apportionment of BrC in cloud water (i.e., Abs_{365}) evaluated by the PMF model (see Supplement for data analysis and evaluation methods) also supports the critical role of aqueous processes on the formation of BrC, as shown in Fig. 4. Factor 1 is associated with relatively higher K^+, NH_4^+, NO_3^-, SO_4^{2-}, and $C_2O_4^{2-}$, contributing 64.3 % to WSOC and 86.9 % to Abs_{365}. It may be appropriately recognized as a secondary product with contribution from biomass burning, as K^+ represents a tracer for biomass burning, and NH_4^+, NO_3^-, $C_2O_4^{2-}$, and SO_4^{2-} are regarded as secondary species (Cheng et al., 2015; Wang et al., 2012). Note that $C_2O_4^{2-}$ is generally considered as a tracer of aqueous-phase processes (Zhang et al., 2017b). As previously observed, the aqueous SOA formed from biomass burning might contributed to the BrC budget in fog water (Gilardoni et al., 2016). Factor 2 is characterized by high levels of crustal trace elements such as Mg^{2+}, Ca^{2+}, Mn, and Zn, and thus identified as crustal materials, contributing 21.9 % to WSOC and 8.7 % to Abs_{365}. Factor 3 shows extremely high loading with Na^+ and relatively high Mg^{2+}, Cl^-, and Ni, which may

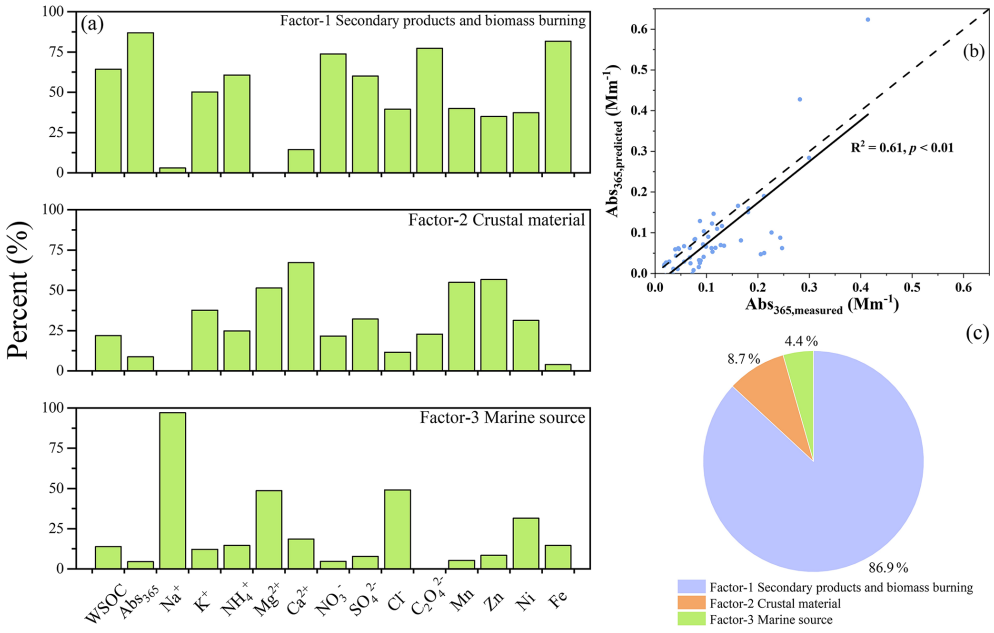

Figure 4. **(a)** The composition profiles (% of each species) for the three factors simulated of cloud water by PMF, and **(b)** the correlation of measured, and predicated Abs_{365}, and **(c)** the source apportionment for Abs_{365} in cloud water.

originate from marine environments, contributing 13.8 % to WSOC and 4.4 % to Abs_{365}.

3.3 Fluorescence properties of BrC in $PM_{2.5}$ and cloud water

The results from the EEMs measurements further indicate the different characteristics of WSOC and WS-BrC in $PM_{2.5}$ and cloud water. Based on the PARAFAC model calculation (Fig. 5), two independent fluorescence components (P1–P2) assigned as humic-like substances are found in $PM_{2.5}$, whereas four independent fluorescence components (C1–C4) assigned as humic-like substances (C1–C3), and tyrosine-like and/or protein-like substances (C4) are found in cloud water (Catalá et al., 2015; Coble, 2007). The fluorescence components of cloud water are similar to those at Mt. Tai (Zhao et al., 2019) and in France (Bianco et al., 2016b), where humic-like and protein-like substances are the main chromophores in cloud water. Compared with $PM_{2.5}$, tyrosine-like and/or protein-like substances are unique to cloud water in the present study, which may partly be due to their relative enrichment in cloud water (Kristensson et al., 2010; Zhang and Anastasio, 2003).

In addition, the relative contribution of individual chromophores indicated by F_{max} in $PM_{2.5}$ and cloud water also exhibits different characteristics, although humic-like substances are the dominant fluorescent fraction in both $PM_{2.5}$ and cloud water. The relative contribution shows no obvious difference between P1 and P2 components in $PM_{2.5}$ (FREE-$PM_{2.5}$ and INT-$PM_{2.5}$), whereas the C3 component contributes the most (40.0 %) to the fluorescent intensity in cloud water. Further analysis of the relationship between the fluorescent components (F_{max}) and the light absorption of WSOC (Abs_{365}) in $PM_{2.5}$ and cloud water shows significant positive correlations between F_{max} of all fluorescent components with Abs_{365} ($r > 0.63$, $p < 0.01$, see Fig. 5). It suggests that these fluorescent components are tightly linked to the light absorption of WSOC. The FI, BIX, and HIX of cloud water are 1.58 ± 0.22, 0.57 ± 0.09, and 4.99 ± 3.83, respectively, which indicates limited humified WSOC in cloud water, and also that it is less affected by microorganisms and local sources (Huguet et al., 2009; McKnight et al., 2001; Zsolnay et al., 1999). Therefore, it is most likely that the organic components in cloud water may be significantly affected by in-cloud aqueous formation, which is consistent with the PMF results. With respect to the secondary processes, humic-like substances may be formed through Maillard reaction involving carbonyls with ammonium or amines (Bones et al., 2010; Hawkins et al., 2016), and also the phototransformation of tyrosine (Berto et al., 2016).

4 Conclusions and implications

In the present study, the light-absorption properties of the cloud RES, cloud INT, and cloud-free particles were simultaneously investigated at a remote mountain site in southern China. Coupled with the measurements of light-absorption and fluorescence properties of WSOC in the collected cloud water and $PM_{2.5}$, it is evident that in-cloud aqueous processing facilitates the formation of BrC (i.e., 67 %–85 % secondary BrC in cloud RES particles by the MSR method). As

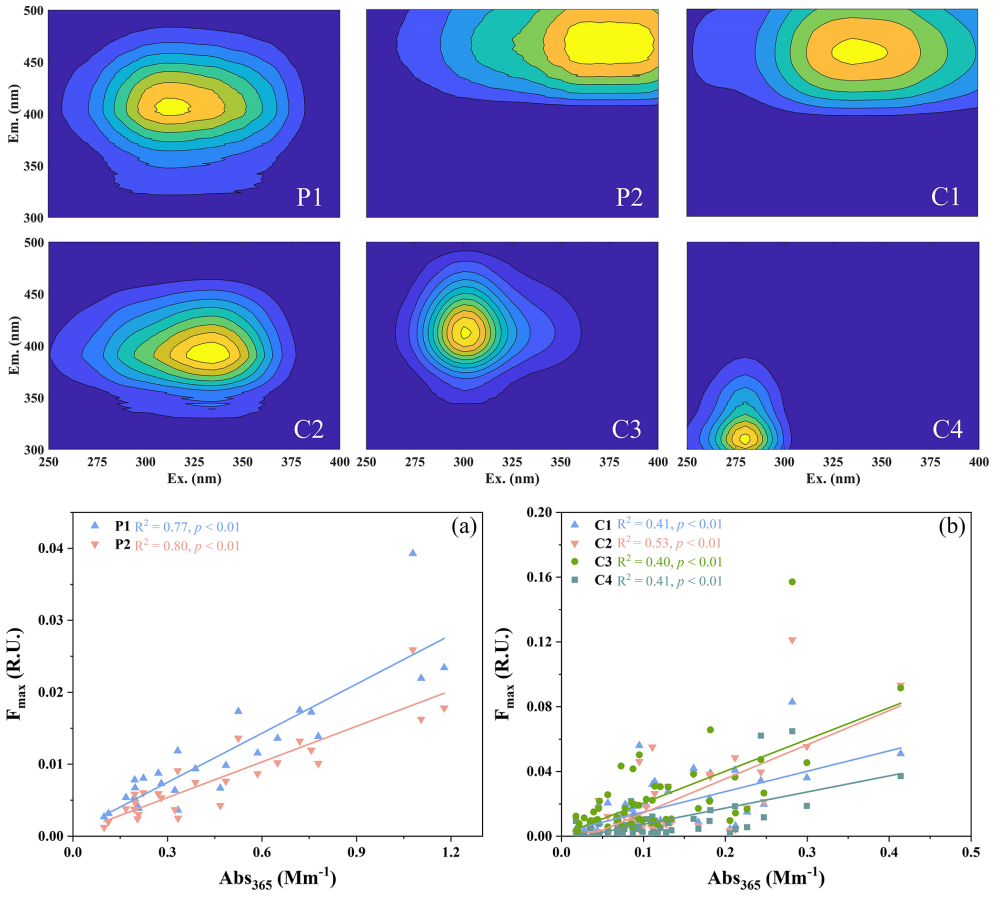

Figure 5. The EEMs components in $PM_{2.5}$ (P1–P2) and cloud water (C1–C4) that were identified by PARAFAC model, and the correlation between each chromophore F_{max} and Abs_{365} in **(a)** $PM_{2.5}$, and **(b)** cloud water.

potential contributors to light absorption of BrC, only two fluorescence fractions of humic-like substances are found in $PM_{2.5}$, whereas four fluorescence fractions (three types of humic-like substances and one type of tyrosine-like and/or protein-like substances) are identified in cloud water, most likely attributed to secondary production. While extensive laboratory evidence indicated the possible formation of BrC in aqueous phase (Hems et al., 2021), our study represents the first attempt to show the possibility under real cloud conditions. The results could support a previous hypothesis that in-cloud formation of BrC might contribute to the enhanced absorption coefficients ratio of BrC to BC in the attitude between 5–12 km (Zhang et al., 2017c). Such a process might also have potential implications for the lifecycle of BrC (Liu et al., 2020).

In order to evaluate the influence of BrC formation in the light-absorption properties of cloud water, the imaginary part of the refractive index for cloud water was calculated according to Gelencsér et al. (2003), as detailed in the Supplement Sect. S1. The average imaginary part of cloud water was 5.5×10^{-8} at 365 nm (Fig. S7) and, ~ 10 times that of pure water. The imaginary part (3.4×10^{-8} at 475 nm) is a magnitude higher than previous laboratory simulation results (5.2×10^{-9} at 475 nm), involving 3,5-dihydroxy-benzoic acid reaction with $FeCl_3$ (Gelencsér et al., 2003). It should also be noted that it is the lowest estimation since only WSOC is included in the calculation. As previously indicated, the overall light absorption of WIOC cannot be negligible. According to the average MAE_{550} and AAE of WSOC in cloud water and INT-$PM_{2.5}$, the optical properties of BrC during cloud events could be classified as weakly absorptive BrC (Saleh, 2020). The measured optical properties and suggested in-cloud formation of BrC would help better understand the atmospheric evolution and the radiation forcing of BrC.

Data availability. All the data can be obtained by contacting the corresponding author.

Supplement. Supporting information includes one text (Sect. S1), seven figures (Figs. S1–S7), and three tables (Tables S1–S3) related to the manuscript. The supplement related to this article is available online at: https://doi.org/10.5194/acp-22-4827-2022-supplement.

Author contributions. XB and GZ designed the research with input from DC, XW, and PP. ZG, XP, WS, XH, and YY collected and analyzed samples. ZG processed data when XH and YY gave constructive discussion. ZG wrote the manuscript, and XB, GZ, and YF interpreted data and edited the manuscript. XH, XP, and WS had an active role in supporting the sampling work. All authors contributed to the discussions of the results and refinement of the manuscript.

Competing interests. The contact author has declared that neither they nor their coauthors have any competing interests.

Disclaimer. Publisher's note: Copernicus Publications remains neutral with regard to jurisdictional claims in published maps and institutional affiliations.

Acknowledgements. This is contribution No. IS-3149 from GIGCAS.

Financial support. This research was supported by the Natural Science Foundation of Guangdong Province (grant no. 2019B151502022), the National Natural Science Foundation of China (grant nos. 42077322, 42130611, and 41877307), the Youth Innovation Promotion Association CAS (grant no. 2021354), and the Guangdong Foundation for Program of Science and Technology Research (grant nos. 2019B121205006 and 2020B1212060053).

Review statement. This paper was edited by Eduardo Landulfo and reviewed by two anonymous referees.

References

Berto, S., De Laurentiis, E., Tota, T., Chiavazza, E., Daniele, P. G., Minella, M., Isaia, M., Brigante, M., and Vione, D.: Properties of the humic-like material arising from the phototransformation of L-tyrosine, Sci. Total Environ., 545–546, 434–444, https://doi.org/10.1016/j.scitotenv.2015.12.047, 2016.

Bianco, A., Voyard, G., Deguillaume, L., Mailhot, G., and Brigante, M.: Improving the characterization of dissolved organic carbon in cloud water: Amino acids and their impact on the oxidant capacity, Sci. Rep., 6, 37420, https://doi.org/10.1038/srep37420, 2016a.

Bianco, A., Passananti, M., Deguillaume, L., Mailhot, G., and Brigante, M.: Tryptophan and tryptophan-like substances in cloud water: Occurrence and photochemical fate, Atmos. Environ., 137, 53–61, https://doi.org/10.1016/j.atmosenv.2016.04.034, 2016b.

Bikkina, S. and Sarin, M.: Brown carbon in the continental outflow to the North Indian Ocean, Environ. Sci. Process. Impacts, 21, 970–987, https://doi.org/10.1039/c9em00089e, 2019.

Birdwell, J. E. and Valsaraj, K. T.: Characterization of dissolved organic matter in fogwater by excitation-emission matrix fluorescence spectroscopy, Atmos. Environ., 44, 3246–3253, https://doi.org/10.1016/j.atmosenv.2010.05.055, 2010.

Bones, D. L., Henricksen, D. K., Mang, S. A., Gonsior, M., Bateman, A. P., Nguyen, T. B., Cooper, W. J., and Nizkorodov, S. A.: Appearance of strong absorbers and fluorophores in limonene-O_3 secondary organic aerosol due to NH_4^+-mediated chemical aging over long time scales, J. Geophys. Res.-Atmos., 115, D05203, https://doi.org/10.1029/2009JD012864, 2010.

Boone, E. J., Laskin, A., Laskin, J., Wirth, C., Shepson, P. B., Stirm, B. H., and Pratt, K. A.: Aqueous Processing of Atmospheric Organic Particles in Cloud Water Collected via Aircraft Sampling, Environ. Sci. Technol., 49, 8523–8530, https://doi.org/10.1021/acs.est.5b01639, 2015.

Brown, H., Liu, X., Feng, Y., Jiang, Y., Wu, M., Lu, Z., Wu, C., Murphy, S., and Pokhrel, R.: Radiative effect and climate impacts of brown carbon with the Community Atmosphere Model (CAM5), Atmos. Chem. Phys., 18, 17745–17768, https://doi.org/10.5194/acp-18-17745-2018, 2018.

Catalá, T. S., Reche, I., Fuentes-Lema, A., Romera-Castillo, C., Nieto-Cid, M., Ortega-Retuerta, E., Calvo, E., Álvarez, M., Marrasé, C., Stedmon, C. A., and Álvarez-Salgado, X. A.: Turnover time of fluorescent dissolved organic matter in the dark global ocean, Nat. Commun., 6, 5986, https://doi.org/10.1038/ncomms6986, 2015.

Chen, Q., Ikemori, F., and Mochida, M.: Light Absorption and Excitation-Emission Fluorescence of Urban Organic Aerosol Components and Their Relationship to Chemical Structure, Environ. Sci. Technol., 50, 10859–10868, https://doi.org/10.1021/acs.est.6b02541, 2016.

Chen, Y., Ge, X., Chen, H., Xie, X., Chen, Y., Wang, J., Ye, Z., Bao, M., Zhang, Y., and Chen, M.: Seasonal light absorption properties of water-soluble brown carbon in atmospheric fine particles in Nanjing, China, Atmos. Environ., 187, 230–240, https://doi.org/10.1016/j.atmosenv.2018.06.002, 2018.

Chen, Y., Xie, X., Shi, Z., Li, Y., Gai, X., Wang, J., Li, H., Wu, Y., Zhao, X., Chen, M., and Ge, X.: Brown carbon in atmospheric fine particles in Yangzhou, China: Light absorption properties and source apportionment, Atmos. Res., 244, 105028, https://doi.org/10.1016/j.atmosres.2020.105028, 2020.

Cheng, C., Wang, G., Meng, J., Wang, Q., Cao, J., Li, J., and Wang, J.: Size-resolved airborne particulate oxalic and related secondary organic aerosol species in the urban atmosphere of Chengdu, China, Atmos. Res., 161–162, 134–142, https://doi.org/10.1016/j.atmosres.2015.04.010, 2015.

Choudhary, V., Rajput, P., Singh, D. K., Singh, A. K., and Gupta, T.: Light absorption characteristics of brown carbon during foggy and non-foggy episodes over the Indo-Gangetic Plain, Atmos. Pollut. Res., 9, 494–501, https://doi.org/10.1016/j.apr.2017.11.012, 2018.

Coble, P. G.: Marine optical biogeochemistry: The chemistry of ocean color, Chem. Rev., 107, 402–418, https://doi.org/10.1021/cr050350+, 2007.

De Haan, D. O., Hawkins, L. N., Kononenko, J. A., Turley, J. J., Corrigan, A. L., Tolbert, M. A., and Jimenez, J. L.: Formation of nitrogen-containing oligomers by methylglyoxal and amines in simulated evaporating cloud droplets, Environ. Sci. Technol., 45, 984–991, https://doi.org/10.1021/es102933x, 2011.

Demoz, B. B., Collett, J. L., and Daube, B. C.: On the caltech active strand cloudwater collectors, Atmos. Res., 41, 47–62, https://doi.org/10.1016/0169-8095(95)00044-5, 1996.

Desyaterik, Y., Sun, Y., Shen, X., Lee, T., Wang, X., Wang, T., and Collett, J. L.: Speciation of "brown" carbon in cloud water impacted by agricultural biomass burning in eastern China, J. Geophys. Res.-Atmos., 118, 7389–7399, https://doi.org/10.1002/jgrd.50561, 2013.

Drinovec, L., Močnik, G., Zotter, P., Prévôt, A. S. H., Ruckstuhl, C., Coz, E., Rupakheti, M., Sciare, J., Müller, T., Wiedensohler, A., and Hansen, A. D. A.: The "dual-spot" Aethalometer: an improved measurement of aerosol black carbon with real-time loading compensation, Atmos. Meas. Tech., 8, 1965–1979, https://doi.org/10.5194/amt-8-1965-2015, 2015.

Ervens, B.: Modeling the Processing of Aerosol and Trace Gases in Clouds and Fogs, Chem. Rev., 115, 4157–4198, https://doi.org/10.1021/cr5005887, 2015.

Fan, X., Wei, S., Zhu, M., Song, J., and Peng, P.: Comprehensive characterization of humic-like substances in smoke $PM_{2.5}$ emitted from the combustion of biomass materials and fossil fuels, Atmos. Chem. Phys., 16, 13321–13340, https://doi.org/10.5194/acp-16-13321-2016, 2016.

Fu, Y., Lin, Q., Zhang, G., Yang, Y., Yang, Y., Lian, X., Peng, L., Jiang, F., Bi, X., Li, L., Wang, Y., Chen, D., Ou, J., Wang, X., Peng, P., Zhu, J., and Sheng, G.: Impact of in-cloud aqueous processes on the chemical compositions and morphology of individual atmospheric aerosols, Atmos. Chem. Phys., 20, 14063–14075, https://doi.org/10.5194/acp-20-14063-2020, 2020.

Gao, Y., Wang, Q., Li, L., Dai, W., Yu, J., Ding, L., Li, J., Xin, B., Ran, W., Han, Y., and Cao, J.: Optical properties of mountain primary and secondary brown carbon aerosols in summertime, Sci. Total Environ., 806, 150570, https://doi.org/10.1016/j.scitotenv.2021.150570, 2022.

Gelencsér, A., Hoffer, A., Kiss, G., Tombácz, E., Kurdi, R., and Bencze, L.: In-situ formation of light-absorbing organic matter in cloud water, J. Atmos. Chem., 45, 25–33, https://doi.org/10.1023/A:1024060428172, 2003.

Gilardoni, S., Massoli, P., Paglione, M., Giulianelli, L., Carbone, C., Rinaldi, M., Decesari, S., Sandrini, S., Costabile, F., Gobbi, G. P., Pietrogrande, M. C., Visentin, M., Scotto, F., Fuzzi, S., and Facchini, M. C.: Direct observation of aqueous secondary organic aerosol from biomass-burning emissions, P. Natl. Acad. Sci. USA, 113, 10013–10018, https://doi.org/10.1073/pnas.1602212113, 2016.

Harrison, M. A. J., Barra, S., Borghesi, D., Vione, D., Arsene, C., and Iulian Olariu, R.: Nitrated phenols in the atmosphere: A review, Atmos. Environ., 39, 231–248, https://doi.org/10.1016/j.atmosenv.2004.09.044, 2005.

Hawkins, L. N., Lemire, A. N., Galloway, M. M., Corrigan, A. L., Turley, J. J., Espelien, B. M., and De Haan, D. O.: Maillard Chemistry in Clouds and Aqueous Aerosol As a Source of Atmospheric Humic-Like Substances, Environ. Sci. Technol., 50, 7443–7452, https://doi.org/10.1021/acs.est.6b00909, 2016.

Heal, M. R., Harrison, M. A. J., and Neil Cape, J.: Aqueous-phase nitration of phenol by N_2O_5 and $ClNO_2$, Atmos. Environ., 41, 3515–3520, https://doi.org/10.1016/j.atmosenv.2007.02.003, 2007.

Hecobian, A., Zhang, X., Zheng, M., Frank, N., Edgerton, E. S., and Weber, R. J.: Water-Soluble Organic Aerosol material and the light-absorption characteristics of aqueous extracts measured over the Southeastern United States, Atmos. Chem. Phys., 10, 5965–5977, https://doi.org/10.5194/acp-10-5965-2010, 2010.

Hems, R. F., Schnitzler, E. G., Liu-Kang, C., Cappa, C. D., and Abbatt, J. P. D.: Aging of Atmospheric Brown Carbon Aerosol, ACS Earth Sp. Chem., 5, 722–748, https://doi.org/10.1021/acsearthspacechem.0c00346, 2021.

Huang, R. J., Yang, L., Shen, J., Yuan, W., Gong, Y., Guo, J., Cao, W., Duan, J., Ni, H., Zhu, C., Dai, W., Li, Y., Chen, Y., Chen, Q., Wu, Y., Zhang, R., Dusek, U., O'Dowd, C., and Hoffmann, T.: Water-Insoluble Organics Dominate Brown Carbon in Wintertime Urban Aerosol of China: Chemical Characteristics and Optical Properties, Environ. Sci. Technol., 54, 7836–7847, https://doi.org/10.1021/acs.est.0c01149, 2020.

Huguet, A., Vacher, L., Relexans, S., Saubusse, S., Froidefond, J. M., and Parlanti, E.: Properties of fluorescent dissolved organic matter in the Gironde Estuary, Org. Geochem., 40, 706–719, https://doi.org/10.1016/j.orggeochem.2009.03.002, 2009.

Kaskaoutis, D. G., Grivas, G., Stavroulas, I., Bougiatioti, A., Liakakou, E., Dumka, U. C., Gerasopoulos, E., and Mihalopoulos, N.: Apportionment of black and brown carbon spectral absorption sources in the urban environment of Athens, Greece, during winter, Sci. Total Environ., 801, 149739, https://doi.org/10.1016/j.scitotenv.2021.149739, 2021.

Kaur, R. and Anastasio, C.: Light absorption and the photoformation of hydroxyl radical and singlet oxygen in fog waters, Atmos. Environ., 164, 387–397, https://doi.org/10.1016/j.atmosenv.2017.06.006, 2017.

Kim, H., Kim, J. Y., Jin, H. C., Lee, J. Y., and Lee, S. P.: Seasonal variations in the light-absorbing properties of water-soluble and insoluble organic aerosols in Seoul, Korea, Atmos. Environ., 129, 234–242, https://doi.org/10.1016/j.atmosenv.2016.01.042, 2016.

Kim, H., Collier, S., Ge, X., Xu, J., Sun, Y., Jiang, W., Wang, Y., Herckes, P., and Zhang, Q.: Chemical processing of water-soluble species and formation of secondary organic aerosol in fogs, Atmos. Environ., 200, 158–166, https://doi.org/10.1016/j.atmosenv.2018.11.062, 2019.

Kirillova, E. N., Marinoni, A., Bonasoni, P., Vuillermoz, E., Facchini, M. C., Fuzzi, S., and Decesari, S.: Light absorption properties of brown carbon in the high Himalayas, J. Geophys. Res., 121, 9621–9639, https://doi.org/10.1002/2016JD025030, 2016.

Kristensen, T. B., Du, L., Nguyen, Q. T., Nøjgaard, J. K., Bender Koch, C., Faurskov Nielsen, O., Hallar, A. G., Lowenthal, D. H., Nekat, B., Van Pinxteren, D., Herrmann, H., Glasius, M., Kjaergaard, H. G., and Bilde, M.: Chemical properties of HULIS from three different environments, J. Atmos. Chem., 72, 65–80, https://doi.org/10.1007/s10874-015-9302-8, 2015.

Kristensson, A., Rosenørn, T., and Bilde, M.: Cloud droplet activation of amino acid aerosol particles, J. Phys. Chem. A, 114, 379–386, https://doi.org/10.1021/jp9055329, 2010.

Lawaetz, A. J. and Stedmon, C. A.: Fluorescence intensity calibration using the Raman scatter peak of water, Appl. Spectrosc., 63, 936–940, https://doi.org/10.1366/000370209788964548, 2009.

Lebedev, A. T., Polyakova, O. V., Mazur, D. M., Artaev, V. B., Canet, I., Lallement, A., Vaïtilingom, M., Deguillaume, L., and Delort, A. M.: Detection of semi-volatile compounds in cloud waters by GC×GC-TOF-MS. Evidence of phenols and phthalates as priority pollutants, Environ. Pollut., 241, 616–625, https://doi.org/10.1016/j.envpol.2018.05.089, 2018.

Li, J., Wang, X., Chen, J., Zhu, C., Li, W., Li, C., Liu, L., Xu, C., Wen, L., Xue, L., Wang, W., Ding, A., and Herrmann, H.: Chemical composition and droplet size distribution of cloud at the sum-

mit of Mount Tai, China, Atmos. Chem. Phys., 17, 9885–9896, https://doi.org/10.5194/acp-17-9885-2017, 2017.

Li, M., Fan, X., Zhu, M., Zou, C., Song, J., Wei, S., Jia, W., and Peng, P.: Abundance and Light Absorption Properties of Brown Carbon Emitted from Residential Coal Combustion in China, Environ. Sci. Technol., 53, 595–603, https://doi.org/10.1021/acs.est.8b05630, 2019.

Lian, X., Zhang, G., Yang, Y., Lin, Q., Fu, Y., Jiang, F., Peng, L., Hu, X., Chen, D., Wang, X., Peng, P., Sheng, G., and Bi, X.: Evidence for the Formation of Imidazole from Carbonyls and Reduced Nitrogen Species at the Individual Particle Level in the Ambient Atmosphere, Environ. Sci. Technol. Lett., 8, 9–15, https://doi.org/10.1021/acs.estlett.0c00722, 2021.

Lin, G., Penner, J. E., Flanner, M. G., Sillman, S., Xu, L., and Zhou, C.: Radiative forcing of organic aerosol in the atmosphere and on snow: Effects of SOA and brown carbon, J. Geophys. Res., 119, 7453–7476, https://doi.org/10.1002/2013JD021186, 2014.

Lin, Q., Zhang, G., Peng, L., Bi, X., Wang, X., Brechtel, F. J., Li, M., Chen, D., Peng, P., Sheng, G., and Zhou, Z.: In situ chemical composition measurement of individual cloud residue particles at a mountain site, southern China, Atmos. Chem. Phys., 17, 8473–8488, https://doi.org/10.5194/acp-17-8473-2017, 2017.

Lin, Y. C., Zhang, Y. L., Xie, F., Fan, M. Y., and Liu, X.: Substantial decreases of light absorption, concentrations and relative contributions of fossil fuel to light-absorbing carbonaceous aerosols attributed to the COVID-19 lockdown in east China, Environ. Pollut., 275, 116615, https://doi.org/10.1016/j.envpol.2021.116615, 2021.

Lin, Y. H., Budisulistiorini, S. H., Chu, K., Siejack, R. A., Zhang, H., Riva, M., Zhang, Z., Gold, A., Kautzman, K. E., and Surratt, J. D.: Light-absorbing oligomer formation in secondary organic aerosol from reactive uptake of isoprene epoxydiols, Environ. Sci. Technol., 48, 12012–12021, https://doi.org/10.1021/es503142b, 2014.

Liu, D., He, C., Schwarz, J. P., and Wang, X.: Lifecycle of light-absorbing carbonaceous aerosols in the atmosphere, npj Clim. Atmos. Sci., 3, 40, https://doi.org/10.1038/s41612-020-00145-8, 2020.

Liu, J., Horowitz, L. W., Fan, S., Carlton, A. G., and Levy, H.: Global in-cloud production of secondary organic aerosols: Implementation of a detailed chemical mechanism in the GFDL atmospheric model AM3, J. Geophys. Res.-Atmos., 117, D15303, https://doi.org/10.1029/2012JD017838, 2012.

Lüttke, J. and Levsen, K.: Phase partitioning of phenol and nitrophenols in clouds, Atmos. Environ., 31, 2649–2655, https://doi.org/10.1016/S1352-2310(96)00228-2, 1997.

McKnight, D. M., Boyer, E. W., Westerhoff, P. K., Doran, P. T., Kulbe, T., and Andersen, D. T.: Spectrofluorometric characterization of dissolved organic matter for indication of precursor organic material and aromaticity, Limnol. Oceanogr., 46, 38–48, https://doi.org/10.4319/lo.2001.46.1.0038, 2001.

Murphy, K. R., Stedmon, C. A., Graeber, D., and Bro, R.: Fluorescence spectroscopy and multi-way techniques. PARAFAC, Anal. Methods, 5, 6557–6566, https://doi.org/10.1039/c3ay41160e, 2013.

Nguyen, T. B., Lee, P. B., Updyke, K. M., Bones, D. L., Laskin, J., Laskin, A., and Nizkorodov, S. A.: Formation of nitrogen- and sulfur-containing light-absorbing compounds accelerated by evaporation of water from secondary organic aerosols, J. Geophys. Res.-Atmos., 117, D01207, https://doi.org/10.1029/2011JD016944, 2012.

Pang, H., Zhang, Q., Lu, X., Li, K., Chen, H., Chen, J., Yang, X., Ma, Y., Ma, J., and Huang, C.: Nitrite-Mediated Photooxidation of Vanillin in the Atmospheric Aqueous Phase, Environ. Sci. Technol., 53, 14253–14263, https://doi.org/10.1021/acs.est.9b03649, 2019.

Park, S. S. and Yu, J.: Chemical and light absorption properties of humic-like substances from biomass burning emissions under controlled combustion experiments, Atmos. Environ., 136, 114–122, https://doi.org/10.1016/j.atmosenv.2016.04.022, 2016.

Perrino, C. and Marcovecchio, F.: A new method for assessing the contribution of Primary Biological Atmospheric Particles to the mass concentration of the atmospheric aerosol, Environ. Int., 87, 108–115, https://doi.org/10.1016/j.envint.2015.11.015, 2016.

Pósfai, M., Gelencsér, A., Simonics, R., Arató, K., Li, J., Hobbs, P. V., and Buseck, P. R.: Atmospheric tar balls: Particles from biomass and biofuel burning, J. Geophys. Res.-Atmos., 109, D06213, https://doi.org/10.1029/2003jd004169, 2004.

Pratt, K. A., Fiddler, M. N., Shepson, P. B., Carlton, A. G., and Surratt, J. D.: Organosulfates in cloud water above the Ozarks' isoprene source region, Atmos. Environ., 77, 231–238, https://doi.org/10.1016/j.atmosenv.2013.05.011, 2013.

Saleh, R.: From Measurements to Models: Toward Accurate Representation of Brown Carbon in Climate Calculations, Curr. Pollut. Reports, 6, 90–104, https://doi.org/10.1007/s40726-020-00139-3, 2020.

Saleh, R., Robinson, E. S., Tkacik, D. S., Ahern, A. T., Liu, S., Aiken, A. C., Sullivan, R. C., Presto, A. A., Dubey, M. K., Yokelson, R. J., Donahue, N. M., and Robinson, A. L.: Brownness of organics in aerosols from biomass burning linked to their black carbon content, Nat. Geosci., 7, 647–650, https://doi.org/10.1038/ngeo2220, 2014.

Satish, R., Rastogi, N., Singh, A., and Singh, D.: Change in characteristics of water-soluble and water-insoluble brown carbon aerosols during a large-scale biomass burning, Environ. Sci. Pollut. Res., 27, 33339–33350, https://doi.org/10.1007/s11356-020-09388-7, 2020.

Seinfeld, J. H. and Pandis, S. N.: Atmospheric Chemistry and Physics: From Air Pollution to Climate Change, John Wiley & Sons, ISBN 978-1-118-94740-1, 2016.

Shapiro, E. L., Szprengiel, J., Sareen, N., Jen, C. N., Giordano, M. R., and McNeill, V. F.: Light-absorbing secondary organic material formed by glyoxal in aqueous aerosol mimics, Atmos. Chem. Phys., 9, 2289–2300, https://doi.org/10.5194/acp-9-2289-2009, 2009.

Shingler, T., Dey, S., Sorooshian, A., Brechtel, F. J., Wang, Z., Metcalf, A., Coggon, M., Mülmenstädt, J., Russell, L. M., Jonsson, H. H., and Seinfeld, J. H.: Characterisation and airborne deployment of a new counterflow virtual impactor inlet, Atmos. Meas. Tech., 5, 1259–1269, https://doi.org/10.5194/amt-5-1259-2012, 2012.

Soleimanian, E., Mousavi, A., Taghvaee, S., Shafer, M. M., and Sioutas, C.: Impact of secondary and primary particulate matter (PM) sources on the enhanced light absorption by brown carbon (BrC) particles in central Los Angeles, Sci. Total Environ., 705, 135902, https://doi.org/10.1016/j.scitotenv.2019.135902, 2020.

Spracklen, D. V., Jimenez, J. L., Carslaw, K. S., Worsnop, D. R., Evans, M. J., Mann, G. W., Zhang, Q., Canagaratna, M. R.,

Allan, J., Coe, H., McFiggans, G., Rap, A., and Forster, P.: Aerosol mass spectrometer constraint on the global secondary organic aerosol budget, Atmos. Chem. Phys., 11, 12109–12136, https://doi.org/10.5194/acp-11-12109-2011, 2011.

Teich, M., van Pinxteren, D., Wang, M., Kecorius, S., Wang, Z., Müller, T., Močnik, G., and Herrmann, H.: Contributions of nitrated aromatic compounds to the light absorption of water-soluble and particulate brown carbon in different atmospheric environments in Germany and China, Atmos. Chem. Phys., 17, 1653–1672, https://doi.org/10.5194/acp-17-1653-2017, 2017.

Vione, D., Maurino, V., Minero, C., and Pelizzetti, E.: Phenol photonitration upon UV irradiation of nitrite in aqueous solution I: Effects of oxygen and 2-propanol, Chemosphere, 45, 893–902, https://doi.org/10.1016/S0045-6535(01)00035-2, 2001.

Vione, D., Maurino, V., Minero, C., Lucchiari, M., and Pelizzetti, E.: Nitration and hydroxylation of benzene in the presence of nitrite/nitrous acid in aqueous solution, Chemosphere, 56, 1049–1059, https://doi.org/10.1016/j.chemosphere.2004.05.027, 2004.

Wang, G., Kawamura, K., Cheng, C., Li, J., Cao, J., Zhang, R., Zhang, T., Liu, S., and Zhao, Z.: Molecular distribution and stable carbon isotopic composition of dicarboxylic acids, ketocarboxylic acids, and α-dicarbonyls in size-resolved atmospheric particles from Xi'an City, China, Environ. Sci. Technol., 46, 4783–4791, https://doi.org/10.1021/es204322c, 2012.

Wang, H., Zhang, L., Huo, T., Wang, B., Yang, F., Chen, Y., Tian, M., Qiao, B., and Peng, C.: Application of parallel factor analysis model to decompose excitation-emission matrix fluorescence spectra for characterizing sources of water-soluble brown carbon in $PM_{2.5}$, Atmos. Environ., 223, 117192, https://doi.org/10.1016/j.atmosenv.2019.117192, 2020.

Wang, Q., Han, Y., Ye, J., Liu, S., Pongpiachan, S., Zhang, N., Han, Y., Tian, J., Wu, C., Long, X., Zhang, Q., Zhang, W., Zhao, Z., and Cao, J.: High Contribution of Secondary Brown Carbon to Aerosol Light Absorption in the Southeastern Margin of Tibetan Plateau, Geophys. Res. Lett., 46, 4962–4970, https://doi.org/10.1029/2019GL082731, 2019a.

Wang, Q., Ye, J., Wang, Y., Zhang, T., Ran, W., Wu, Y., Tian, J., Li, L., Zhou, Y., Hang Ho, S. S., Dang, B., Zhang, Q., Zhang, R., Chen, Y., Zhu, C., and Cao, J.: Wintertime Optical Properties of Primary and Secondary Brown Carbon at a Regional Site in the North China Plain, Environ. Sci. Technol., 53, 12389–12397, https://doi.org/10.1021/acs.est.9b03406, 2019b.

Wang, Q., Liu, H., Wang, P., Dai, W., Zhang, T., Zhao, Y., Tian, J., Zhang, W., Han, Y., and Cao, J.: Optical source apportionment and radiative effect of light-absorbing carbonaceous aerosols in a tropical marine monsoon climate zone: the importance of ship emissions, Atmos. Chem. Phys., 20, 15537–15549, https://doi.org/10.5194/acp-20-15537-2020, 2020.

Wang, Q., Wang, L., Tao, M., Chen, N., Lei, Y., Sun, Y., Xin, J., Li, T., Zhou, J., Liu, J., Ji, D., and Wang, Y.: Exploring the variation of black and brown carbon during COVID-19 lockdown in megacity Wuhan and its surrounding cities, China, Sci. Total Environ., 791, 148226, https://doi.org/10.1016/j.scitotenv.2021.148226, 2021.

Weishaar, J. L., Aiken, G. R., Bergamaschi, B. A., Fram, M. S., Fujii, R., and Mopper, K.: Evaluation of specific ultraviolet absorbance as an indicator of the chemical composition and reactivity of dissolved organic carbon, Environ. Sci. Technol., 37, 4702–4708, https://doi.org/10.1021/es030360x, 2003.

Wu, C. and Yu, J. Z.: Determination of primary combustion source organic carbon-to-elemental carbon (OC / EC) ratio using ambient OC and EC measurements: secondary OC-EC correlation minimization method, Atmos. Chem. Phys., 16, 5453–5465, https://doi.org/10.5194/acp-16-5453-2016, 2016.

Wu, C., Wu, D., and Yu, J. Z.: Quantifying black carbon light absorption enhancement with a novel statistical approach, Atmos. Chem. Phys., 18, 289–309, https://doi.org/10.5194/acp-18-289-2018, 2018.

Wu, C., Wang, G., Li, J., Li, J., Cao, C., Ge, S., Xie, Y., Chen, J., Li, X., Xue, G., Wang, X., Zhao, Z., and Cao, F.: The characteristics of atmospheric brown carbon in Xi'an, inland China: sources, size distributions and optical properties, Atmos. Chem. Phys., 20, 2017–2030, https://doi.org/10.5194/acp-20-2017-2020, 2020.

Wu, G., Ram, K., Fu, P., Wang, W., Zhang, Y., Liu, X., Stone, E. A., Pradhan, B. B., Dangol, P. M., Panday, A. K., Wan, X., Bai, Z., Kang, S., Zhang, Q., and Cong, Z.: Water-Soluble Brown Carbon in Atmospheric Aerosols from Godavari (Nepal), a Regional Representative of South Asia, Environ. Sci. Technol., 53, 3471–3479, https://doi.org/10.1021/acs.est.9b00596, 2019.

Yang, J., Au, W. C., Law, H., Lam, C. H., and Nah, T.: Formation and evolution of brown carbon during aqueous-phase nitrate-mediated photooxidation of guaiacol and 5-nitroguaiacol, Atmos. Environ., 254, 118401, https://doi.org/10.1016/j.atmosenv.2021.118401, 2021.

Yang, Y., Lin, Q., Fu, Y., Lian, X., Jiang, F., Peng, L., Zhang, G., Li, L., Chen, D., Li, M., Ou, J., Bi, X., Wang, X., and Sheng, G.: Stage-resolved in-cloud scavenging of submicron and BC-containing particles: A case study, Atmos. Environ., 244, 117883, https://doi.org/10.1016/j.atmosenv.2020.117883, 2021.

Zhang, G., Lin, Q., Peng, L., Bi, X., Chen, D., Li, M., Li, L., Brechtel, F. J., Chen, J., Yan, W., Wang, X., Peng, P., Sheng, G., and Zhou, Z.: The single-particle mixing state and cloud scavenging of black carbon: a case study at a high-altitude mountain site in southern China, Atmos. Chem. Phys., 17, 14975–14985, https://doi.org/10.5194/acp-17-14975-2017, 2017a.

Zhang, G., Lin, Q., Peng, L., Yang, Y., Fu, Y., Bi, X., Li, M., Chen, D., Chen, J., Cai, Z., Wang, X., Peng, P., Sheng, G., and Zhou, Z.: Insight into the in-cloud formation of oxalate based on in situ measurement by single particle mass spectrometry, Atmos. Chem. Phys., 17, 13891–13901, https://doi.org/10.5194/acp-17-13891-2017, 2017b.

Zhang, Q. and Anastasio, C.: Free and combined amino compounds in atmospheric fine particles ($PM_{2.5}$) and fog waters from Northern California, Atmos. Environ., 37, 2247–2258, https://doi.org/10.1016/S1352-2310(03)00127-4, 2003.

Zhang, Q., Shen, Z., Zhang, L., Zeng, Y., Ning, Z., Zhang, T., Lei, Y., Wang, Q., Li, G., Sun, J., Westerdahl, D., Xu, H., and Cao, J.: Investigation of Primary and Secondary Particulate Brown Carbon in Two Chinese Cities of Xi'an and Hong Kong in Wintertime, Environ. Sci. Technol., 54, 3803–3813, https://doi.org/10.1021/acs.est.9b05332, 2020.

Zhang, Q., Shen, Z., Zhang, T., Kong, S., Lei, Y., Wang, Q., Tao, J., Zhang, R., Wei, P., Wei, C., Cui, S., Cheng, T., Ho, S. S. H., Li, Z., Xu, H., and Cao, J.: Spatial distribution and sources of winter black carbon and brown carbon in six Chinese megacities, Sci. Total Environ., 762, 143075, https://doi.org/10.1016/j.scitotenv.2020.143075, 2021.

Zhang, Y., Forrister, H., Liu, J., DIbb, J., Anderson, B., Schwarz, J. P., Perring, A. E., Jimenez, J. L., Campuzano-Jost, P., Wang, Y., Nenes, A., and Weber, R. J.: Top-of-atmosphere radiative forcing affected by brown carbon in the upper troposphere, Nat. Geosci., 10, 486–489, https://doi.org/10.1038/ngeo2960, 2017.

Zhao, W., Fu, P., Yue, S., Li, L., Xie, Q., Zhu, C., Wei, L., Ren, H., Li, P., Li, W., Sun, Y., Wang, Z., Kawamura, K., and Chen, J.: Excitation-emission matrix fluorescence, molecular characterization and compound-specific stable carbon isotopic composition of dissolved organic matter in cloud water over Mt. Tai, Atmos. Environ., 213, 608–619, https://doi.org/10.1016/j.atmosenv.2019.06.034, 2019.

Zhu, C. S., Qu, Y., Huang, H., Chen, J., Dai, W. T., Huang, R. J., and Cao, J. J.: Black Carbon and Secondary Brown Carbon, the Dominant Light Absorption and Direct Radiative Forcing Contributors of the Atmospheric Aerosols Over the Tibetan Plateau, Geophys. Res. Lett., 48, e2021GL092524, https://doi.org/10.1029/2021GL092524, 2021.

Zhuang, B. L., Liu, L., Shen, F. H., Wang, T. J., and Han, Y.: Semidirect radiative forcing of internal mixed black carbon cloud droplet and its regional climatic effect over China, J. Geophys. Res.-Atmos., 115, D00K19, https://doi.org/10.1029/2009JD013165, 2010.

Zsolnay, A., Baigar, E., Jimenez, M., Steinweg, B., and Saccomandi, F.: Differentiating with fluorescence spectroscopy the sources of dissolved organic matter in soils subjected to drying, Chemosphere, 38, 45–50, https://doi.org/10.1016/S0045-6535(98)00166-0, 1999.